buildings

MDPI

Article

Modeling Compressive and Flexural Strength of Cement Grouts with Fly Ash, Silica Fume, and Polyethylene Terephthalate: A Correlated Multivariate Regression Approach in Compositional Data Analysis

Omar Almutairi and Muhammad Imran Khan *

Civil Engineering Department, College of Engineering, Imam Mohammad Ibn Saud Islamic University (IMSIU), Riyadh 11423, Saudi Arabia; oalhjlih@imamu.edu.sa
* Correspondence: mekhan@imamu.edu.sa

Abstract

An integrated statistical–graphical framework is introduced for designing sustainable cement grout mixes that incorporate polyethylene terephthalate (PET) waste and supplementary cementitious materials (SCMs) for semi-flexible pavement applications. A correlated multivariate linear mixed-effects model employs additive log-ratio transformations of PET and SCM proportions (fly ash or silica fume relative to cement) to predict 1-day, 7-day, and 28-day compressive strengths and 28-day flexural strength within a single unified framework. This approach quantifies both the systematic strength penalty of PET substitution and the benefits of SCM additions. The model results demonstrate high random-intercept correlations, substantial reductions in the Akaike information criterion (AIC) and root mean squared error (RMSE) compared to a null model, and marginal and conditional coefficient of determination (R^2) values of 0.96 and 0.99, respectively, confirming major capture of the variance in the mechanical response. Complementary ternary plots visualize predicted 28-day performance across the cement–PET–SCM compositional space. These plots reveal that zero-PET formulations along the cement–binder edge achieve maximum strengths, with both fly ash and silica fume maximizing compressive and flexural strengths and any PET addition uniformly degrading performance. By combining rigorous compositional modeling with intuitive visualization, the proposed framework offers quantitative rigor, practical mix design guidelines, and a scalable protocol for optimizing sustainable grout formulations and informing future exploration of alternative fillers, flow regimes, and durability assessments.

Keywords: cement grouts; compressive strength; flexural strength; flow value; modeling; computational data analysis

check for updates

Academic Editor: Gabriele Milani

Received: 25 September 2025
Revised: 20 October 2025
Accepted: 29 October 2025
Published: 4 November 2025

Citation: Almutairi, O.; Khan, M.I. Modeling Compressive and Flexural Strength of Cement Grouts with Fly Ash, Silica Fume, and Polyethylene Terephthalate: A Correlated Multivariate Regression Approach in Compositional Data Analysis. *Buildings* **2025**, *15*, 3976. https://doi.org/10.3390/buildings15213976

Copyright: © 2025 by the authors. Licensee MDPI, Basel, Switzerland. This article is an open access article distributed under the terms and conditions of the Creative Commons Attribution (CC BY) license (https://creativecommons.org/licenses/by/4.0/).

1. Background Study

In response to growing concerns about environmental degradation, researchers have been increasingly exploring the incorporation of industrial byproducts and waste materials into construction materials. The cement industry is responsible for nearly 8% of global carbon dioxide (CO_2) emissions, stemming from both fuel combustion and the calcination of limestone [1,2]. The production of one ton of Portland cement consumes approximately 2.8 tons of raw materials and energy, further intensifying resource depletion and environmental pollution [3,4]. To address these challenges, there is a worldwide push to adopt

sustainable alternatives that can partially or completely replace traditional materials, such as ordinary Portland cement (OPC), particularly for applications in which cement plays a dominant role, such as in cement grout [5].

Within pavement engineering, sustainability efforts have focused on developing eco-friendly grouting materials that achieve the desired mechanical performance while minimizing the environmental impact. Various waste-derived materials, such as glass waste powder (GWP) [6], ceramic waste powder (CWP) [7], palm frond waste ash (PFWA) [8], and polyethylene terephthalate (PET) waste [9], have been tested as partial cement replacements. One promising material is paper sludge ash (PSA), a byproduct of the paper recycling industry. The UK alone produces 4.5 million tons of paper annually, 73% of which comes from recovered fiber, generating significant waste during the deinking and treatment stages [10]. Research has shown that PSA can be used as a supplementary cementitious material in concrete and pavement structures, enhancing strength performance while promoting waste reuse [11]. For instance, Devi et al. [12] reported improved compressive, split tensile, and flexural strengths at up to 5% PSA replacement, supporting its use as a sustainable cement alternative.

Building upon these advances, semi-flexible pavements (also known as grouted macadam) have attracted growing attention for their ability to integrate the advantages of both flexible and rigid systems. A semi-flexible pavement is composed of an open-graded asphalt framework that is filled with a highly flowable cementitious grout [13–16]. This structure combines the flexibility of asphalt with the rigidity of concrete, providing a durable, jointless surface suitable for quick opening to traffic, often within 24 h. Compared to rigid pavements, semi-flexible pavements cost less and are more adaptable [14]. The construction process for grouted macadam consists of two phases, including first, laying an open-graded asphalt mixture and then infusing cement grout into its voids under gravity. Various grouting materials have been tested for this application, including cement paste, polymer-modified mortars, rubber-modified mortars, engineered cement composites, and high-performance cement paste [17–20]. OPC remains a common base, often modified with silica fume, fly ash, or superplasticizers to optimize workability, strength, and flow [21,22].

Although semi-flexible pavements differ structurally from conventional semi-rigid systems, they exhibit similar degradation mechanisms such as fatigue and shrinkage cracking, which can compromise long-term durability. Fatigue damage in cement-treated layers has been identified as a primary failure mode affecting service life [23,24], while shrinkage in cement-treated or recycled mixtures may induce cracking and accelerate deterioration [25]. Such issues parallel those reported in semi-rigid bases used for low-volume or stabilized pavements [26]. Therefore, ensuring adequate grout fluidity is critical—if it is too low, the asphalt skeleton may not be fully filled, leading to weak bonding and early distress [27].

To meet these performance requirements sustainably, researchers have experimented with modifying grout compositions using various supplementary and recycled materials. Superplasticizers, silica fume, and fly ash are commonly used to balance flowability and strength [21,22]. Superplasticizers can enhance flowability without increasing the water–cement ratio, although higher doses may reduce the mechanical strength [28]. Most technical guidelines suggest a fluidity range of 11–16 s, with a minimum 7-day compressive strength of 10–30 MPa and flexural strength of approximately 3 MPa [21,29–34]. Further research continues to focus on developing sustainable and cost-effective grout formulations that maintain these mechanical and workability benchmarks while incorporating waste-based components such as PSA, marble dust, palm frond ash, and PET [35–41].

The utilization of waste plastics, particularly PET in cement-based materials and its influence on mechanical properties, has been explored in several studies. In concrete

applications, waste plastics are often used either as fibers or as partial replacements for fine and coarse aggregates [42], particularly to develop lightweight concrete [43]. Incorporating recycled PET fibers has been shown to improve concrete's tensile strength and resistance to cracking [44,45]. However, replacing aggregates or sand with PET beyond 10% by volume significantly reduces compressive strength [46,47]. Some studies have also examined the partial replacement of cement with PET, reporting compressive strength reductions of up to 23% and 72% at 5% and 20% replacement levels, respectively [48]. Schaefer et al. [49] found similar reductions but noted that gamma-irradiated PET combined with fly ash (FA) or silica fume (SF) improved strength. Other studies have confirmed that gamma-irradiated waste plastics enhance the strength of cementitious grouts [50–52]. These findings demonstrate that achieving the right synergy between plastic-based waste and supplementary cementitious materials (SCMs) is crucial for optimizing both sustainability and mechanical performance.

The increasing diversity of such materials has made the formulation of grouts inherently multicomponent and compositional in nature. The proportions of cement, PET, and SCMs form a closed-sum system, which complicates traditional statistical analysis. Conventional regression methods often fail to capture the dependency structure among mixture components, potentially leading to biased or misleading conclusions [53]. To address this, the field has increasingly adopted compositional data analysis (CoDA) principles. A study demonstrated the efficacy of log-ratio transformations (e.g., isometric log-ratio, ILR; additive log-ratio, ALR) in cement and concrete science, allowing for the unbiased assessment of how a change in one component proportionally affects the entire mixture and its properties [54]. Given that key performance indicators such as compressive strength, flexural strength, and workability are often measured simultaneously and are intrinsically correlated, univariate models provide an incomplete picture. Research conducted on predictive modeling of mechanical properties of concrete, evaluating workability properties using the slump cone method and strength properties through compressive, split tensile, and flexural strength tests. Their study underscores the significance of multivariate modeling in assessing multiple concrete properties simultaneously [55]. The combination of CoDA and multivariate mixed-effects models, as employed in this study, represents a sophisticated advancement. This approach acknowledges both the compositional nature of the input variables and the correlated, hierarchical structure of the experimental outcome data, thereby providing a robust and statistically sound framework for optimizing complex grout and concrete formulations. This approach is particularly valuable for optimizing modern formulations that incorporate recycled and secondary materials.

Accordingly, the objective of this study is to develop a robust statistical framework for predicting and optimizing the mechanical performance of cementitious grouts incorporating polyethylene terephthalate (PET) and supplementary cementitious materials (SCMs) such as fly ash or silica fume. To achieve this goal, this work offers two key innovations. First, it formulates and validates a correlated multivariate linear mixed-effects model that integrates additive log-ratio transformations for PET and SCMs to predict 1-, 7-, and 28-day compressive strengths and 28-day flexural strength within a unified framework. Second, it couples these quantitative estimates with ternary plots that map 28-day performance across the cement–PET–binder compositional space, thereby translating complex model outputs into intuitive mix design guidelines. Together, these contributions not only demonstrate methodological rigor but also provide practical tools for optimizing sustainable grout formulations.

2. Data Collection and Methodology

2.1. Experimentation

The materials used to prepare the cement grouts included ordinary Portland cement (type-1 and obtained from local vendor), powdered waste PET (procured from local waste recycling factor), SCMs such as fly ash (type -C and supplied by local supplier) and silica fume (powdery byproduct in electric arc furnaces), and a superplasticizer. Drawing from the authors' previous research, a superplasticizer dosage of 1% and a water–cement (w/c) ratio of 0.35 were selected [50,56]. These values ensured that the grout achieved a flow time between 11 and 16 s, which is ideal for effectively filling the voids in open-graded asphalt mixtures to form semi-flexible pavement surfaces. Powdered waste PET with particle sizes under 150 μm and SCMs were incorporated at varying levels, ranging from 0% to 10% of the cement's weight. All grout mixtures were prepared according to the ASTM C305 standard [57]. To evaluate the fresh grout's flowability, a flow cone test was conducted in accordance with ASTM C939 [58]. Cube samples measuring 50 mm × 50 mm × 50 mm were cast and subjected to compressive strength testing at 1, 7, and 28 days. The samples were loaded at a rate of 0.90 kN/s using an ELE Universal Testing Machine (UTM) with a 3000-kN capacity, in accordance with ASTM C109 [59]. Flexural strength tests were performed on beam specimens sized 40 mm × 40 mm × 160 mm after 28 days of curing. These tests were conducted using a 2000-kN ELE-UTM, in accordance with ASTM C348 [60]. A center-point loading setup was used, with a loading rate of 0.05 kN/s.

2.2. Compositional Structure and Data Preparation

The dataset comprises observations of grout mixes formulated for semi-flexible pavement applications. For each mix, 16 samples were produced, and the proportion of each component was recorded as a percentage of the total mix. The study includes 12 mixes composed of fly ash, cement, and powdered polyethylene terephthalate (PET); 12 mixes composed of silica fume, cement, and powdered PET; and one control mix composed only of cement and powdered PET. The flow value, measured in seconds, was recorded prior to casting the grout samples. Compressive strength in megapascals (MPa) was measured at 1, 7, and 28 days, whereas flexural strength was measured only at 28 days. This dataset facilitated a comparative analysis of how varying proportions of supplementary cementing materials influence the performance of the grouts (see Table 1). SD is the standard deviation in Table 1.

Table 1. Descriptive Statistics Summary.

Variable	Mean	Range	SD
Response variables			
1-day compressive strength (MPa)	16.64	5.64–33.32	7.62
7-day compressive strength (MPa)	34.92	19.19–61.81	9.65
28-day compressive strength (MPa)	51.85	33.64–82.54	11.73
28-day flexural strength (MPa)	7.19	5.43–9.98	1.04
Predictor variables			
Flow value (s)	16.54	9.1–26	4.16
Cement (%)	90	80–100	5.32
Polyethylene terephthalate (%)	5.2	0–10	3.62
Fly ash (%)	2.6	0–10	4.05
Silica fume (%)	2.2	0–10	3.50

Since the sum of all components is fixed at 100%, any increase in one component must be counterbalanced by a decrease in another, creating an inherent dependency among the variables. This feature of compositional data can distort conventional analyses if

not properly addressed. An ALR transformation, which converts each component into its logarithmic ratio relative to a chosen reference—cement, in this case—was employed to overcome this problem. This transformation effectively removes the constant-sum constraint, enabling the use of standard statistical methods to assess the relationships among the materials accurately [61]. Table 2 presents the ALR-transformed values for the 15 unique grout mix compositions. To address the mathematical constraint that the natural logarithm of zero is undefined, zero values in the original dataset were replaced with a small positive constant (0.000001) prior to transformation. This substitution ensures numerical stability while preserving the relative structure of the compositions.

Table 2. Additive Log-Ratio Transformed Compositional Values of Grout Mix Designs.

Mix No	Cement (%)	PET (%)	FA or SF (%)	ALR_PET [ln (PET/Cement)]	ALR_FA/SF [ln ((FA or SF)/Cement)]
1	100	0	0	−18.42	−18.42
2	97.5	2.5	0	−3.66	−18.40
3	95	5	0	−2.94	−18.37
4	92.5	7.5	0	−2.51	−18.34
5	90	10	0	−2.20	−18.32
6	95	0	5	−18.37	−2.94
7	92.5	2.5	5	−3.61	−2.92
8	90	5	5	−2.89	−2.89
9	87.5	7.5	5	−2.46	−2.86
10	85	10	5	−2.14	−2.83
11	90	0	10	−18.32	−2.20
12	87.5	2.5	10	−3.56	−2.17
13	85	5	10	−2.83	−2.14
14	82.5	7.5	10	−2.40	−2.11
15	80	10	10	−2.08	−2.08

Cement was adopted as the reference denominator in the ALR transformation because it constitutes the chemically active base component that anchors all replacement effects. This choice ensures direct interpretability of log--ratios as strength variations relative to the reactive cement fraction. Sensitivity analysis using total binder as the alternative reference confirmed that model coefficients preserved both sign and magnitude, indicating robustness to reference choice.

2.3. Statistical Modeling: Multivariate Linear Mixed Model

To accommodate four correlated, continuous outcomes measured for each grout mix, the conventional multilevel framework was extended to a multivariate setting. Let y_{h_ij} denote the hth outcome (h = 1,. . .,4) for the ith sample in mix j. Each response is modeled as the sum of fixed effects, mix-level random intercepts, and residual error:

$$y_{h_ij} = X_{h_ij} \cdot \beta_h + \mu_{hj} + \varepsilon_{h_ij} \quad (1)$$

Here:

- X_{h_ij} is the 1 × p vector of fixed-effect predictors (e.g., ALR log-ratios, flow value).
- β_h is the p × 1 coefficient vector for the hth outcome.
- μ_{hj} is the random intercept for outcome h in mix j, capturing between-mix variability.
- ε_{h_ij} is the within-mix residual error.

The four random intercepts for mix j are collected in $\mu_j = (\mu_{1j}, \ldots, \mu_{4j})^T$ and assumed to follow a multivariate normal (MVN) distribution with mean zero and covariance Ψ, thus allowing outcomes to covary across mixes:

$$\mu_j \sim \text{MVN}(0, \Psi) \quad (2)$$

Similarly, residuals within each sample, $\varepsilon_{ij} = (\varepsilon_{1ij}, \ldots, \varepsilon_{4ij})^T$, are assumed MVN (0, Σ), with Σ capturing within-mix correlations and measurement noise:

$$\varepsilon_{ij} \sim \text{MNV}(0, \Sigma) \quad (3)$$

Together, Equations (1)–(3) define a two-level multivariate linear mixed-effects model in which level 1 consists of "outcomes" nested within level 2 "mixes." Parameter estimation was performed by maximum likelihood using the glmmTMB package in R, employing a Laplace approximation to integrate over random effects [62].

3. Results and Discussion

3.1. Multivariate Linear Mixed Model

Multivariate linear mixed model estimates are first presented to quantify how grout composition and curing age govern both compressive and flexural strength gains. The model results are then complemented by ternary plots of predicted 28-day compressive or flexural strengths that correspond to different mixes of cement, PET, and supplementary binders (fly ash or silica fume) within the acceptable flow value range.

Table 3 presents detailed estimates from the correlated multivariate regression model for four strength outcomes: compressive strength (CS) at 1, 7, and 28 days and flexural strength (FS) at 28 days. The fixed-effect intercepts increase as expected with curing time, from 10.08 MPa at 1 day (Z = 6.39) to 32.82 MPa at 7 days (Z = 16.84) and 51.61 MPa at 28 days (Z = 19.35), demonstrating the progressive development of matrix cohesion under standard hydration conditions. The ALR_PET coefficient is negative and highly significant across all CS measurements: −0.95 (Z = −10.00) at 1 day, −1.08 (Z = −9.22) at 7 days, and −1.10 (Z = −6.85) at 28 days, indicating that increasing PET substitution systematically decreases both early and later compressive strength. A similar, though smaller, reduction is seen for flexural strength, with an estimate of −0.04 (Z = −1.70) at 28 days, confirming that PET also slightly compromises tensile--bending performance. In contrast, the ALR_FA/SF coefficient exerts a consistent and growing positive effect on strength gain. Its effect on CS increases from 0.19 (Z = 2.07) at 1 day to 0.60 (Z = 5.44) at 7 days and 0.91 (Z = 6.00) at 28 days, underscoring the pronounced benefit of SCMs over time. For flexural strength, the same log-ratio produces a 0.07 (Z = 3.09) gain at 28 days, highlighting the measurable reinforcement achieved by fly ash or silica fume additions. In addition, the binary silica-fume indicator—flagging instances in which the FA/SF log-ratio refers specifically to silica fume—fails to reach statistical significance but reveals a clear temporal trend. For CS, its coefficient shifts from −0.89 (Z = −1.59) at 1 day to −0.09 (Z = 0.76) at 7 days and 0.61 (Z = 0.84) at 28 days, suggesting that while the direct FA-versus-SF contrast remains imprecise early on, silica fume may gradually outperform fly ash in later CS development. In FS, the SF indicator yields 0.21 (Z = 1.39) at 28 days, suggesting a modest bending--tension advantage of silica fume when viewed together with the strong ALR_FA/SF term. The flow-value indicator (11–16 s) significantly enhances only the 1-day compressive response, with an increase of 3.16 (Z = 2.60), and loses relevance at 7 and 28 days (Z = 1.38 and 1.69 for CS; Z = 0.55 for FS). This transient effect suggests that early workability influences initial setting strength but has little bearing on longer-term mechanical properties. At the mix level, random intercepts for the three CS outcomes

exhibit very high pairwise correlations—r = 0.88 between 1- and 7-day CS, r = 0.88 between 1- and 28-day CS, and r = 0.93 between 7- and 28-day CS—validating the decision to model these endpoints jointly. Model diagnostics confirm superior performance relative to the null specification: the AIC decreases from 2854.5 to 1705.2, the RMSE decreases from 3.68 to 1.44, and the marginal coefficient of determination (R^2) is 0.96 for fixed effects alone and 0.99 when random effects are included, demonstrating both excellent explanatory power and predictive accuracy.

Table 3. Multivariate Linear Mixed Model Results.

Outcomes, MPa	**1-Day CS (7-Day CS)**			**28-Day CS (28-Day FS)**		
Fixed Parameter	**Estimate**	**Std. Error**	**Z-Stat**	**Estimate**	**Std. Error**	**Z-Stat**
Intercept	10.08 (32.82)	1.58 (1.95)	6.39 (16.84)	51.61 (7.61)	2.67 (0.42)	19.35 (18.20)
ALR_PET	−0.95 (−1.08)	0.10 (0.12)	−10.00 (−9.22)	−1.10 (−0.04)	0.16 (0.03)	−6.85 (−1.70)
ALR_FA/SF	0.19 (0.60)	0.09 (0.11)	2.07 (5.44)	0.91 (0.07)	0.15 (0.02)	6.00 (3.09)
Flow value indicator	3.16 (2.07)	1.22 (1.50)	2.6 (1.38)	3.48 (0.18)	2.06 (0.32)	1.69 (0.55)
Silica fume indicator	−0.89 (0.52)	0.56 (0.69)	−1.59 (0.76)	0.80 (0.21)	0.95 (0.15)	0.84 (1.39)
Random parameter						
Standard deviation of the intercept		2.83 (3.54)			4.90 (---)	
Correlation between Intercepts	1d-CS and 7d-CS	0.88	1d-CS and 28d-CS	0.88	7d-CS and 28d-CS	0.93
Goodness-of-fit measure		Null Model			This Model	
Deviance		2844.5			1651.2	
Degrees of freedom		5			27	
AIC		2854.5			1705.2	
BIC		2874.4			1813	
Accuracy		Fixed-Effect Model Only			This Model	
R^2		0.96			0.99	
RMSE		3.68			1.44	

ALR_PET, Additive log-ratio of powdered polyethylene terephthalate to cement percentages; ALR_FA/SF, additive log-ratio of fly ash or silica fume to cement percentages; AIC, Akaike's information criterion; BIC, Bayesian information criterion; R^2, the coefficient of determination, which reflects the proportion of the total variance in the observed data that is explained by the model's predicted values; RMSE, root mean squared error.

Figures 1–4 illustrate the predicted 28-day compressive strength (CS) and flexural strength (FS) for grout mixtures within the acceptable flow value range, plotted on ternary diagrams whose apexes represent cement, PET, and either fly ash (Figures 1 and 2) or silica fume (Figures 3 and 4). Along the right edge—where PET = 0%—substituting 10% cement with fly ash increases CS from 56.83 MPa to 83.65 MPa and FS from 7.23 MPa to 8.41 MPa. Under the same conditions, 10% silica fume yields CS = 72.85 MPa and FS = 7.96 MPa. These comparisons show that, at zero PET, fly ash produces both the greatest compressive and flexural strengths. Moving inward toward the PET corner reveals a uniform decline in strength as PET content increases. In the fly ash mixes, a mixture with 85% cement, 10% FA, and 5% PET achieves CS = 58.60 MPa and FS = 7.76 MPa, which fall to 48.23 MPa and 7.68 MPa at 85% cement, 5% FA, and 10% PET and then increase slightly to 50.66 MPa and 7.73 MPa at 80% cement, 10% FA, and 10% PET. The silica fume mixes follow a parallel trend: CS and FS decrease from 63.57 MPa/7.31 MPa at 85% cement, 10% SF, and 5% PET to 44.48 MPa/7.09 MPa at 85% cement, 5% SF, and 10% PET before rebounding to 46.26 MPa/7.30 MPa at 80% cement, 10% SF, and 10% PET. This pattern confirms that PET consistently undermines both compressive and flexural performance, regardless of the supplementary binder. Together, these plots demonstrate that the optimal 28-day strength

occurs along the cement–binder edge with PET held to zero and that any PET addition—whether in a fly ash or silica fume system—leads to measurable reductions in both CS and FS. Minimizing PET content is therefore essential for maximizing the mechanical performance of these grout mixtures.

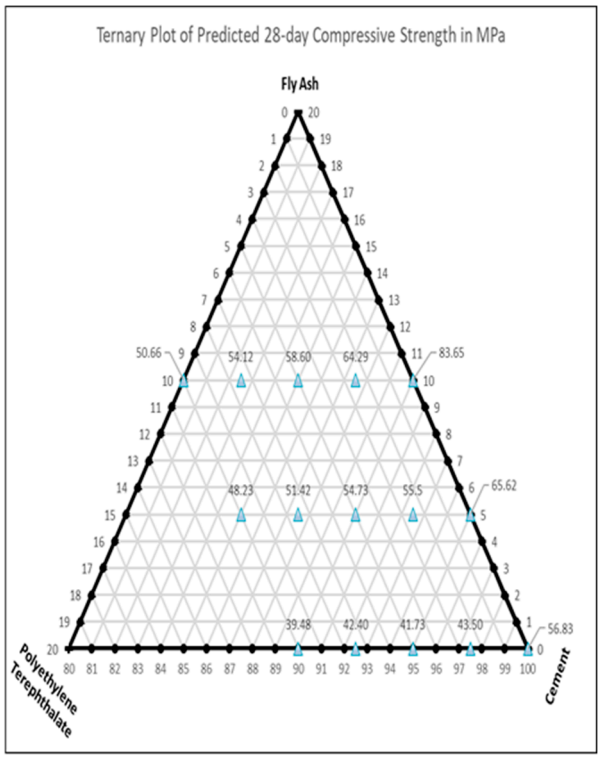


Figure 1. Ternary Diagram—Predicted 28-Day CS (Fly Ash, PET, Cement).

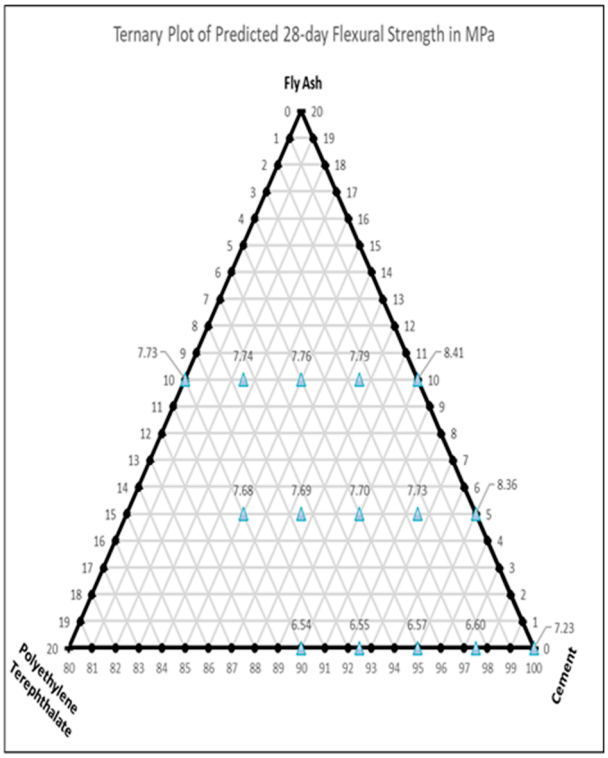


Figure 2. Ternary Diagram—Predicted 28-Day FS (Fly Ash, PET, Cement).

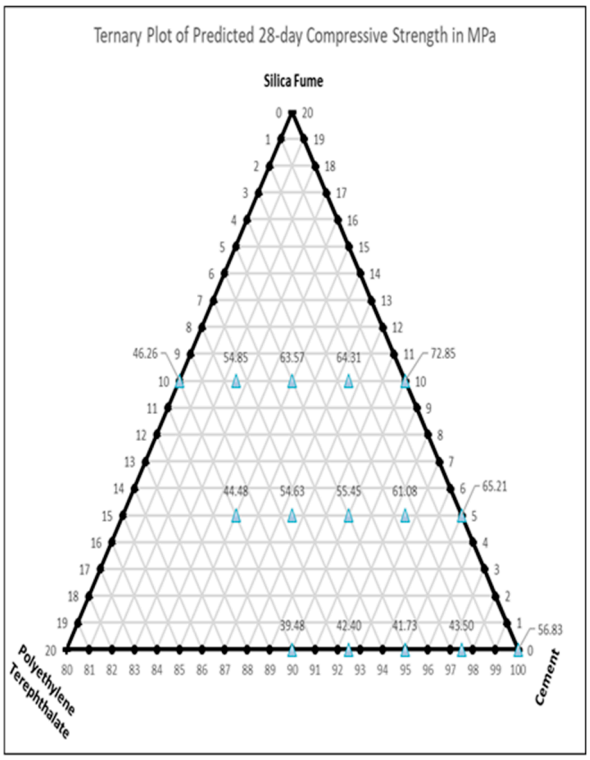


Figure 3. Ternary Diagram—Predicted 28-Day CS (Silica Fume, PET, Cement).

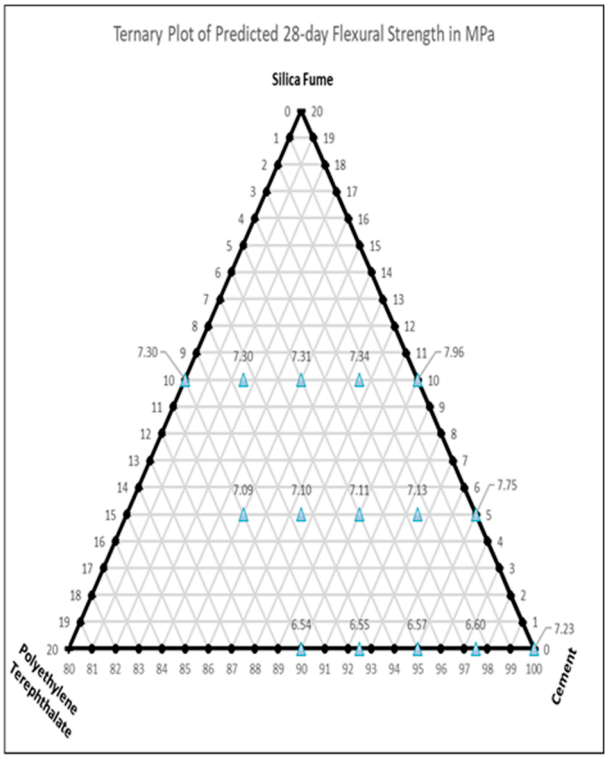


Figure 4. Ternary Diagram—Predicted 28-Day FS (Silica Fume, PET, Cement).

For context, previous studies on cementitious grouts have primarily used univariate regression or response surface methodology (RSM) to predict compressive or flexural strength based on mix proportions [14,46,56]. Such approaches, however, generally ignore the compositional constraint that the total binder content equals 100%, which may lead to biased parameter estimation. In contrast, the present model applies additive log-ratio (ALR)

transformation to handle the closed-sum nature of the mixture and employs a multivariate regression framework to statistically evaluate the effects of cement, PET, and SCMs (fly ash or silica fume) on strength. This formulation provides a more robust and scale-invariant interpretation of how varying each component influences the overall performance, while achieving higher predictive accuracy (RMSE = 1.44; R^2 = 0.99) compared with typical RSM-based models (RMSE ≈ 3–5 MPa).

3.2. Combined Graphical Analyses

Combined statistical and graphical analyses highlight the pivotal roles of PET substitution and supplementary cementitious materials in driving both early-age and 28-day strength development. These insights offer a clear roadmap for tailoring grout formulations to achieve targeted mechanical performance.

Figures 1–4 display ternary plots depicting the predicted 28-day compressive and flexural strengths of cementitious grouts designed for semi-flexible pavement applications. The mix design employed a constant water-to-cement (w/c) ratio of 0.35 along with 1% superplasticizer to ensure adequate workability. The proportions of cement, fly ash (FA), silica fume (SF), and polyethylene terephthalate (PET) were systematically varied, with PET and FA/SF replacing cement by up to 10% by weight.

The complete dataset was used in developing the predictive models for compressive and flexural strength to capture the full range of material behavior. However, since semi-flexible pavement applications require grouts with specific flowability, only those mixtures that achieved flow values within the acceptable range of 11 to 16 s, as determined using the flow cone test, were visualized using ternary diagrams. Therefore, Figures 1–4 selectively present the modeled compressive and flexural strength predictions for grout mixes that satisfied the flow criterion for semi-flexible pavement systems.

3.2.1. Influence of PET and Fly Ash on Compressive and Flexural Strength

The ternary plot in Figure 1 presents the predicted 28-day compressive strength (in MPa) of cementitious grouts prepared for semi-flexible pavement applications. The predicted data indicate that the highest compressive strength (83.65 MPa) was achieved with a formulation containing 10% fly ash, 0% PET, and 90% cement. This clearly suggests that fly ash, within the explored limits, positively contributes to long-term strength when used as a partial cement replacement, likely due to its pozzolanic reactivity and refined particle packing. In contrast, mixtures containing higher percentages of PET generally exhibited lower compressive strengths. For example, samples with PET near or above 8% and low fly ash content showed strengths in the range of 39–43 MPa. This trend suggests that PET, being chemically inert and less reactive, may contribute as a filler without contributing to the hydration process, thereby diluting the binder matrix. Intermediate strength values (e.g., 54.12 to 64.29 MPa) were obtained in formulations where moderate amounts of fly ash and PET were used simultaneously (e.g., 5% FA and 5% PET). While not maximizing strength, these combinations might present an optimal trade-off between mechanical performance and sustainability goals. The inclusion criterion based on the flow range (11–16 s) had a direct influence on the dataset. Mixtures falling outside this flow range—likely due to excessive PET content (leading to high viscosity) or low paste fluidity—were excluded from strength testing. This constraint ensures the practical applicability of the grout in semi-flexible pavements, in which adequate flow is critical for void filling in the porous asphalt skeleton. As expected, mixtures with higher cement contents (above 90%) generally outperformed others, especially when combined with fly ash instead of PET. This is consistent with cement's established role as the primary strength-contributing

binder and supports limiting PET substitution to very small percentages to maintain mechanical integrity.

The ternary plot in Figure 2 illustrates the predicted 28-day flexural strength of cement grouts incorporating PET and fly ash. Overall, the influence of these additives on flexural strength shows the following trend: moderate replacement of cement with fly ash (up to 10%) results in a slight increase in flexural strength. The highest strength (8.41 MPa) was observed at around 10% fly ash and 0% PET. This improvement can be attributed to the pozzolanic reaction of fly ash, which enhances the microstructure and contributes to better stress distribution under flexural loading. Increasing PET content tends to reduce flexural strength. Mixtures with high PET content ($\geq$8%) show lower values (as low as 6.54 MPa). Since PET is a non-reactive, hydrophobic material, it does not contribute to the hydration process and may act as a weak inclusion within the matrix, reducing load transfer efficiency under bending stress. Mixes with balanced PET and fly ash proportions (e.g., 5% each) show intermediate flexural strengths (~7.68–7.76 MPa), suggesting that fly ash may partially compensate for the adverse effects of PET on flexural performance.

These findings support the partial replacement of cement with fly ash up to 10% without compromising the structural strength necessary for semi-flexible pavement applications. However, PET inclusion should be approached cautiously and ideally kept below 5%, especially if strength is a primary concern. Future work should investigate the microstructural interaction of PET particles within the cementitious matrix, as well as the long-term durability of such grouts.

3.2.2. Influence of PET and Silica Fume on Compressive and Flexural Strength

Figure 3 is a ternary plot showing the predicted 28-day compressive strength (MPa) of cement grouts incorporating polyethylene terephthalate (PET) and silica fume (SF), intended for semi-flexible pavement applications. The highest compressive strength (72.85 MPa) was obtained with a mix containing approximately 10% SF, 0% PET, and 90% cement. This affirms the beneficial role of silica fume, which, due to its high pozzolanic activity and ultrafine particle size, enhances the microstructure by densifying the matrix and contributing to additional calcium silicate hydrate (C-S-H) formation. As in the fly ash scenario, mixes with higher PET content (particularly $\geq$8%) demonstrated significantly lower strengths (e.g., 39.48–43.50 MPa). This further corroborates PET's largely inert nature in cementitious systems, in which it primarily acts as a filler and may disrupt the continuity of the cement matrix. Mixes containing moderate proportions of both SF and PET (e.g., 5% each) achieved compressive strengths between 53 and 61 MPa. While these values do not represent the peak performance, they indicate that a balanced ternary blend can still meet acceptable mechanical thresholds while promoting sustainability through reduced cement usage. The inclusion of only those mixtures with acceptable flow times emphasizes the importance of workability in practical applications. Grouts must possess sufficient fluidity to penetrate the porous asphalt skeleton in semi-flexible pavements, and excessive PET content may adversely affect flowability, leading to mix exclusion. When compared to the fly ash-based system (Figure 1), silica fume appears to produce marginally lower peak compressive strengths (72.85 MPa vs. 83.65 MPa). However, the overall strength distribution is tighter and more consistent in the SF system, indicating more predictable performance. This may be due to SF's higher specific surface area and rapid reactivity compared to fly ash.

Figure 4 shows the ternary plot of predicted 28-day flexural strength (in MPa) of cement grouts developed for semi-flexible pavement applications. The incorporation of silica fume leads to a clear improvement in flexural strength. The highest value (7.96 MPa) was obtained with a mix containing 10% silica fume and 0% PET. This increase is attributable to

silica fume's high pozzolanic reactivity and ultrafine particle size, which enhance the bond strength within the matrix and densify the microstructure—factors critical in improving tensile and flexural performance. As observed in the compressive strength results, PET addition has a diminishing effect on flexural strength. Mixes with high PET content ($\geq$8%) exhibited the lowest flexural strength values (as low as 6.54 MPa). This is due to PET's non-cementitious and hydrophobic nature, which leads to weak interfacial bonding and potentially induces microvoids or stress concentrations, especially under bending stresses. Mixtures with moderate amounts of both PET and SF (e.g., 5% each) yielded flexural strength values in the range of 7.09–7.31 MPa. These results suggest that silica fume can compensate, to some extent, for the negative effects of PET through matrix refinement and improved load distribution.

Compared to the fly ash system (Figure 2), the silica fume system exhibits slightly lower peak flexural strength but more consistent performance across different mix ratios. This reflects silica fume's predictable behavior due to its uniform particle size and reactivity, as opposed to fly ash, the performance of which is often more variable, depending on its source and fineness. The ternary plot confirms that silica fume is effective in enhancing the flexural strength of cement grouts, particularly when used without PET. Although PET reduces flexural performance, limited amounts ($\leq$5%) in combination with silica fume may still yield acceptable results for semi-flexible pavement applications, supporting a balance between strength and sustainability. These findings can guide material optimization when incorporating industrial byproducts into cementitious grouts.

The findings reinforce the role of silica fume as an effective partial cement replacement in high-strength grout formulations for semi-flexible pavements. Its contribution to compressive strength is more consistent across various mix compositions than fly ash. However, the use of PET should be minimized or combined strategically with reactive SCMs such as SF to offset its diluting effect. These insights are valuable for developing durable, sustainable grouts tailored for in situ pavement void-filling applications.

4. Conclusions

The proposed multivariate linear mixed-effects model uniquely integrates compositional log-ratios with correlated strength outcomes at multiple ages, enabling simultaneous estimation of 1-day, 7-day, and 28-day compressive strength and 28-day flexural strength. By applying additive log-ratio transformations for PET and supplementary cementitious materials (fly ash or silica fume), the model quantifies both the detrimental impact of PET substitution and the time-dependent benefits of SCM mixes within a single statistical framework. High random-intercept correlations and sharply reduced AIC and RMSE relative to the null specification demonstrate superior explanatory power and predictive accuracy, while the marginal R^2 values of 0.96 (fixed effects) and 0.99 (full model) confirm near-complete capture of the variance in the mechanical response.

Complementing these estimates, ternary plots map predicted 28-day performance across the cement–PET–SCM compositional space within the acceptable flow range. These visualizations reveal that zero-PET mixtures along the cement–binder edge achieve peak strengths—fly ash and silica fume both maximize compressive and flexural strengths—while any PET addition uniformly reduces both compressive and flexural properties. The combined statistical and graphical approach thus provides both quantitative rigor and practical guidance, offering mix-design engineers a clear roadmap for selecting cement/SCM/PET proportions that optimize 28-day mechanical performance.

By combining advanced compositional modeling with intuitive ternary visualization, this work establishes a versatile framework for designing sustainable grout formulations. Future extensions may leverage this framework to explore additional waste-derived fillers,

alternative flow regimes, or long-term durability metrics, thereby broadening its application to emerging materials and performance criteria.

Future research should focus on extending this correlated multivariate modeling approach to include long-term durability metrics, microstructural characterization, and field validation using a wider range of waste-derived constituents and curing regimes.

Author Contributions: Conceptualization, O.A.; methodology, O.A.; software, O.A.; validation, O.A. and M.I.K.; formal analysis, O.A.; investigation, O.A. and M.I.K.; resources, O.A. and M.I.K.; data curation, O.A. and M.I.K.; writing—original draft preparation, O.A. and M.I.K.; writing—review and editing, O.A. and M.I.K.; visualization, O.A. and M.I.K.; supervision, O.A. and M.I.K.; project administration, O.A. and M.I.K.; funding acquisition, O.A. and M.I.K. All authors have read and agreed to the published version of the manuscript.

Funding: This work was supported and funded by the Deanship of Scientific Research at Imam Mohammad Ibn Saud Islamic University (IMSIU) (grant number IMSIU-DDRSP2502).

Data Availability Statement: Data is available on reasonable request from the corresponding author.

Conflicts of Interest: The authors declare no conflicts of interest.

References

1. Van Oss, H.G.; Padovani, A.C. Cement manufacture and the environment: Part I: Chemistry and technology. *J. Ind. Ecol.* **2002**, *6*, 89–105. [CrossRef]
2. Dunuweera, S.; Rajapakse, R. Cement types, composition, uses and advantages of nanocement, environmental impact on cement production, and possible solutions. *Adv. Mater. Sci. Eng.* **2018**, *2018*, 1–11. [CrossRef]
3. Al-Atroush, M.E.; Marouf, A.; Aloufi, M.; Marouf, M.; Sebaey, T.A.; Ibrahim, Y.E. Structural performance assessment of geothermal asphalt pavements: A comparative experimental study. *Sustainability* **2022**, *14*, 12855. [CrossRef]
4. Naik, T.R. Sustainability of the cement and concrete industries. In *Sustainable Construction Materials and Technologies*; CRC Press: Boca Raton, FL, USA, 2020; pp. 19–25.
5. da Rocha Gomes, S.; Ferrara, L.; Sánchez, L.; Moreno, M.S. A comprehensive review of cementitious grouts: Composition, properties, requirements and advanced performance. *Constr. Build. Mater.* **2023**, *375*, 130991. [CrossRef]
6. Yin, W.; Li, X.; Sun, T.; Chen, Y.; Xu, F.; Yan, G.; Xu, M.; Tian, K. Utilization of waste glass powder as partial replacement of cement for the cementitious grouts with superplasticizer and viscosity modifying agent binary mixtures: Rheological and mechanical performances. *Constr. Build. Mater.* **2021**, *286*, 122953. [CrossRef]
7. Al-Nawasir, R.I.; Al-Humeidawi, B.H. Efficient use of ceramic waste powder in Cementitious Grout for the Development of Sustainable Semi-Flexible Pavement Surfaces. *IOP Conf. Ser. Earth Environ. Sci.* **2023**, *1232*, 012039. [CrossRef]
8. Albusaisi, K.M.; Al-Busaltan, S.F.; Kadhim, M.A. Characterizing the Mechanical Properties of Sustainable Modified Cementitious Grout for Semi-Flexible Mixture. *IOP Conf. Ser. Earth Environ. Sci.* **2021**, *856*, 012047. [CrossRef]
9. Khan, M.I.; Sutanto, M.H.; Napiah, M.B.; Zoorob, S.E.; Al-Sabaeei, A.M.; Rafiq, W.; Ali, M.; Memon, A.M. Investigating the mechanical properties and fuel spillage resistance of semi-flexible pavement surfacing containing irradiated waste PET based grouts. *Constr. Build. Mater.* **2021**, *304*, 124641. [CrossRef]
10. Spathi, C. *Novel Applications for Paper Sludge Ash*; Imperial College London: London, UK, 2015.
11. Mavroulidou, M.; Feruku, B.; Boulouki, G. Properties of structural concrete with high-strength cement mixes containing waste paper sludge ash. *J. Mater. Cycles Waste Manag.* **2022**, *24*, 1317–1332. [CrossRef]
12. Devi, P.K.; Sanchaya, M.; Harikaran, M.; Krishna, J.G.; Kaviyarasan, V.; Venkatesh, N. Effective utilization of waste paper sludge ash as a supplementary material for cement. *Mater. Today Proc.* **2023**, *in press*. [CrossRef]
13. Ghahremani, M.; Aghayan, I.; Hosseini, S.A.; Lu, Q.; Behzadian, R. Laboratory assessment of the impact of modified asphalt binder on mechanical properties of grouted macadam mixtures under various performance conditions. *Int. J. Pavement Eng.* **2024**, *25*, 2347986. [CrossRef]
14. Khan, M.N.; Khan, M.I.; Khan, J.H.; Ahmad, S.; Azfar, R.W. Exploring waste marble dust as an additive in cementitious grouts for semi-flexible pavement applications: Analysis and optimization using RSM. *Constr. Build. Mater.* **2024**, *411*, 134554. [CrossRef]
15. Khan, M.I.; Khan, N.; Hashmi, S.R.Z.; Yazid, M.R.M.; Yusoff, N.I.M.; Azfar, R.W.; Ali, M.; Fediuk, R. Prediction of compressive strength of cementitious grouts for semi-flexible pavement application using machine learning approach. *Case Stud. Constr. Mater.* **2023**, *19*, e02370. [CrossRef]
16. Hassani, A.; Taghipoor, M.; Karimi, M.M. A state of the art of semi-flexible pavements: Introduction, design, and performance. *Constr. Build. Mater.* **2020**, *253*, 119196. [CrossRef]

17. Zarei, S.; Ouyang, J.; Yang, W.; Zhao, Y. Experimental analysis of semi-flexible pavement by using an appropriate cement asphalt emulsion paste. *Constr. Build. Mater.* **2020**, *230*, 116994. [CrossRef]
18. Luo, S.; Yang, X.; Zhong, K.; Yin, J. Open-graded asphalt concrete grouted by latex modified cement mortar. *Road Mater. Pavement Des.* **2020**, *21*, 61–77. [CrossRef]
19. Cai, X.; Huang, W.; Wu, K. Study of the self-healing performance of semi-flexible pavement materials grouted with engineered cementitious composites mortar based on a non-standard test. *Materials* **2019**, *12*, 3488. [CrossRef]
20. Bharath, G.; Shukla, M.; Nagabushana, M.; Chandra, S.; Shaw, A. Laboratory and field evaluation of cement grouted bituminous mixes. *Road Mater. Pavement Des.* **2020**, *21*, 1694–1712. [CrossRef]
21. Gong, M.; Xiong, Z.; Chen, H.; Deng, C.; Chen, X.; Yang, J.; Zhu, H.; Hong, J. Evaluation on the cracking resistance of semi-flexible pavement mixture by laboratory research and field validation. *Constr. Build. Mater.* **2019**, *207*, 387–395. [CrossRef]
22. Al-Zerejawy, H.K.; Al-Humeidawi, B.H. Evaluation of the performance of semi-flexible pavement contained sustainable grout material. *AIP Conf. Proc.* **2024**, *3079*, 060019. [CrossRef]
23. Jitsangiam, P.; Nusit, K.; Chummuneerat, S.; Chindaprasirt, P.; Pichayapan, P. Fatigue Assessment of Cement-Treated Base for Roads: An Examination of Beam-Fatigue Tests. *J. Mater. Civ. Eng.* **2016**, *28*, 04016095. [CrossRef]
24. Fedrigo, W.; Heller, L.F.; Brito, L.A.T.; Núñez, W.P. Fatigue of Cold Recycled Cement-Treated Pavement Layers: Experimental and Modeling Study. *Sustainability* **2023**, *15*, 7816. [CrossRef]
25. Fedrigo, W.; Kleinert, T.R.; Núñez, W.P.; Graeff, Â.G.; Pinto da Silva Filho, L.C.; Brito, L.A.T. Shrinkage of Cold Recycled Cement-Treated Mixtures of Asphalt Pavement Materials. *J. Test. Eval.* **2023**, *51*, 2230–2244. [CrossRef]
26. Chakrabarti, S.; Kodikara, J. Basaltic Crushed Rock Stabilized with Cementitious Additives: Compressive Strength and Stiffness, Drying Shrinkage, and Capillary Flow Characteristics. *Transp. Res. Rec.* **2003**, *1819*, 18–26. [CrossRef]
27. Raza, M.S.; Sharma, S.K. A review of mechanical and durability properties and microstructure of semi-flexible pavement. *Innov. Infrastruct. Solut.* **2024**, *9*, 83. [CrossRef]
28. Al-Nawasir, R.; Al-Humeidawi, B.; Shubbar, A. Influence of Sustainable Grout Material on the Moisture Damage of Semi-Flexible Pavement. *Period. Polytech. Civ. Eng.* **2024**, *68*, 3. [CrossRef]
29. Corradini, A.; Cerni, G.; D'Alessandro, A.; Ubertini, F. Improved understanding of grouted mixture fatigue behavior under indirect tensile test configuration. *Constr. Build. Mater.* **2017**, *155*, 910–918. [CrossRef]
30. Afonso, M.L.; Dinis-Almeida, M.; Pereira-de-Oliveira, L.A.; Castro-Gomes, J.; Zoorob, S.E. Development of a semi-flexible heavy duty pavement surfacing incorporating recycled and waste aggregates–Preliminary study. *Constr. Build. Mater.* **2016**, *102*, 155–161. [CrossRef]
31. Saboo, N.; Ranjeesh, R.; Gupta, A.; Suresh, M. Development of hierarchical ranking strategy for the asphalt skeleton in semi-flexible pavement. *Constr. Build. Mater.* **2019**, *201*, 149–158. [CrossRef]
32. Pei, J.; Cai, J.; Zou, D.; Zhang, J.; Li, R.; Chen, X.; Jin, L. Design and performance validation of high-performance cement paste as a grouting material for semi-flexible pavement. *Constr. Build. Mater.* **2016**, *126*, 206–217. [CrossRef]
33. Hou, S.; Xu, T.; Huang, K. Aggregate gradation influence on grouting results and mix design of asphalt mixture skeleton for semi-flexible pavement. *J. Test. Eval.* **2017**, *45*, 591–600. [CrossRef]
34. Yang, B.; Weng, X. The influence on the durability of semi-flexible airport pavement materials to cyclic wheel load test. *Constr. Build. Mater.* **2015**, *98*, 171–175. [CrossRef]
35. Chen, Z.; Qiao, J.; Yang, X.; Sun, Y.; Sun, D. A review of grouting materials for pouring semi-flexible pavement: Materials, design and performance. *Constr. Build. Mater.* **2023**, *379*, 131235. [CrossRef]
36. Elmrabet, R.; El Harfi, A.; El Youbi, M.S. Study of properties of fly ash cements. *Mater. Today Proc.* **2019**, *13*, 850–856. [CrossRef]
37. Nistratov, A.V.; Klimenko, N.N.; Pustynnikov, I.V.; Vu, L.K. Thermal regeneration and reuse of carbon and glass fibers from waste composites. *Emerg. Sci. J.* **2022**, *6*, 967–984. [CrossRef]
38. Liu, W.; Jiang, Y.; Zhao, Z.; Du, R.; Li, H. Material innovation and performance optimization of multi-solid waste-based composite grouting materials for semi-flexible pavements. *Case Stud. Constr. Mater.* **2022**, *17*, e01624. [CrossRef]
39. Hlail, S.H.; Al-Busaltan, S.; Shaban, A.M. Durability Evaluation: Sustainable Semi-flexible Pavement Mixtures. *IOP Conf. Ser. Mater. Sci. Eng.* **2021**, *1067*, 012076. [CrossRef]
40. Mohsen, K.; Al-Busaltan, S.; Kadhim, M.A. Cracking Evaluation of Semi-Flexible Mixture Comparison Sustainable Modified Cementitious Grout. *Kerbala J. Eng. Sci.* **2021**, *1*, 216–232. [CrossRef]
41. Khan, M.I. Robust prediction models for flow and compressive strength of sustainable cement grouts for grouted macadam pavement using RSM. *Constr. Build. Mater.* **2024**, *448*, 138205. [CrossRef]
42. Alani, A.H.; Bunnori, N.M.; Noaman, A.T.; Majid, T.A. Durability performance of a novel ultra-high-performance PET green concrete (UHPPGC). *Constr. Build. Mater.* **2019**, *209*, 395–405. [CrossRef]
43. Choi, Y.W.; Moon, D.J.; Kim, Y.J.; Lachemi, M. Characteristics of mortar and concrete containing fine aggregate manufactured from recycled waste polyethylene terephthalate bottles. *Constr. Build. Mater.* **2009**, *23*, 2829–2835. [CrossRef]

44. Fraternali, F.; Ciancia, V.; Chechile, R.; Rizzano, G.; Feo, L.; Incarnato, L. Experimental study of the thermo-mechanical properties of recycled PET fiber-reinforced concrete. *Compos. Struct.* **2011**, *93*, 2368–2374. [CrossRef]
45. Borg, R.P.; Baldacchino, O.; Ferrara, L. Early age performance and mechanical characteristics of recycled PET fibre reinforced concrete. *Constr. Build. Mater.* **2016**, *108*, 29–47. [CrossRef]
46. Marzouk, O.Y.; Dheilly, R.M.; Queneudec, M. Valorization of post-consumer waste plastic in cementitious concrete composites. *Waste Manag.* **2007**, *27*, 310–318. [CrossRef] [PubMed]
47. Remadnia, A.; Dheilly, R.M.; Laidoudi, B.; Quéneudec, M. Use of animal proteins as foaming agent in cementitious concrete composites manufactured with recycled PET aggregates. *Constr. Build. Mater.* **2009**, *23*, 3118–3123. [CrossRef]
48. Silva, D.A.; Betioli, A.M.; Gleize, P.J.P.; Roman, H.R.; Gómez, L.A.; Ribeiro, J.L.D. Degradation of recycled PET fibers in Portland cement-based materials. *Cem. Concr. Res.* **2005**, *35*, 1741–1746. [CrossRef]
49. Schaefer, C.E.; Kupwade-Patil, K.; Ortega, M.; Soriano, C.; Büyüköztürk, O.; White, A.E.; Short, M.P. Irradiated recycled plastic as a concrete additive for improved chemo-mechanical properties and lower carbon footprint. *Waste Manag.* **2018**, *71*, 426–439. [CrossRef] [PubMed]
50. Khan, M.I.; Sutanto, M.H.; Napiah, M.B.; Khan, K.; Rafiq, W. Design optimization and statistical modeling of cementitious grout containing irradiated plastic waste and silica fume using response surface methodology. *Constr. Build. Mater.* **2021**, *271*, 121504. [CrossRef]
51. Khan, M.I.; Wen, L.S.; Sutanto, M.H.; Napiah, M.B.; Zoorob, S. Effect of cement grouts containing irradiated polyethylene terephthalate on properties of semi-flexible mixtures. *Key Eng. Mater.* **2021**, *888*, 3–8. [CrossRef]
52. Khan, M.I.; Sutanto, M.H.; Khan, K.; Iqbal, M.; Napiah, M.B.; Zoorob, S.E.; Klemeš, J.J.; Bokhari, A.; Rafiq, W. Effective use of recycled waste PET in cementitious grouts for developing sustainable semi-flexible pavement surfacing using artificial neural network (ANN). *J. Clean. Prod.* **2022**, *340*, 130840. [CrossRef]
53. Filzmoser, P.; Hron, K.; Templ, M. *Applied Compositional Data Analysis*; Springer: Berlin/Heidelberg, Germany, 2018.
54. Ferraris, C.F.; Hackley, V.A.; Avilés, A.I.; Buchanan, C. Analysis of the ASTM Round-Robin test on particle size distribution of portland cement: Phase I. *Natl. Inst. Stand. Technol. Rep.* **2002**, *6883*, 1–60.
55. Rajiv, K.N.; Reddy, Y.R.; Kumar, G.S.; Ramaraju, H.K. Predictive modelling of mechanical properties of concrete using machine learning with secondary treated waste water and fly ash. *Clean. Waste Syst.* **2025**, *11*, 100296. [CrossRef]
56. Khan, M.I.; Sutanto, M.H.; Napiah, M.B.; Zoorob, S.E.; Yusoff, N.I.M.; Usman, A.; Memon, A.M. Irradiated polyethylene terephthalate and fly ash based grouts for semi-flexible pavement: Design and optimisation using response surface methodology. *Int. J. Pavement Eng.* **2022**, *23*, 2515–2530. [CrossRef]
57. *ASTMC-305-14*; Standard Practice for Mechanical Mixing of Hydraulic Cement Pastes and Mortars of Plastic Consistency. ASTM International: West Conshohocken, PA, USA, 2003.
58. *ASTM, C939*; Standard Test Method for Flow of Grout for Preplaced-Aggregate Concrete (Flow Cone Method). ASTM International: West Conshohocken, PA, USA, 2002.
59. *ASTM-C109*; Standard Test Method for Compressive Strength of Hydraulic Cement Mortars. ASTM International: West Conshohocken, PA, USA, 2008.
60. *ASTM C348*; Standard Test Method for Flexural Strength of Hydraulic-Cement Mortars. ASTM International: West Conshohocken, PA, USA, 2021.
61. Smithson, M.; Broomell, S.B. Compositional data analysis tutorial. *Psychol. Methods* **2024**, *29*, 362. [CrossRef] [PubMed]
62. Brooks, M.E.; Kristensen, K.; Van Benthem, K.J.; Magnusson, A.; Berg, C.W.; Nielsen, A.; Skaug, H.J.; Mächler, M.; Bolker, B.M. glmmTMB balances speed and flexibility among packages for zero-inflated generalized linear mixed modeling. *R J.* **2017**, *9*, 378–400. [CrossRef]

Disclaimer/Publisher's Note: The statements, opinions and data contained in all publications are solely those of the individual author(s) and contributor(s) and not of MDPI and/or the editor(s). MDPI and/or the editor(s) disclaim responsibility for any injury to people or property resulting from any ideas, methods, instructions or products referred to in the content.